Hemoglobin Allostery: Resonance Raman Spectroscopy of Kinetic Intermediates

Vasanthi Jayaraman, Kenton R. Rodgers, Ishita Mukerji, Thomas G. Spiro*

The end states, R and T, of the allosteric transition in hemoglobin (Hb) are structurally well characterized, but there is little information on intermediate structures along the allosteric pathway. These intermediates were examined by means of time-resolved resonance Raman spectroscopy in the nanosecond-to-microsecond interval after HbCO photolysis. Complementary spectra of the heme group and of the tyrosine and tryptophan residues were recorded during laser excitation at 436 and 230 nanometers. These spectra reveal a sequence of interleaved tertiary and quaternary motions during the photocycle, motions involving the proximal and distal helices, and the $\alpha_1\beta_2$ subunit interface. This sequence leads to a modified form of the T state, in which the $\alpha_1\beta_2$ interface is deformed as a result of two carbon monoxide molecules binding to the same dimer within the tetramer.

Allostery, the process by which proteins change their shape upon binding small molecules or ions, is used by nature to control numerous biological functions, including muscle contraction, metabolic regulation, and transport of oxygen in the blood (*1*). For several proteins, x-ray crystallography has provided atomic resolution structures of the end states of allosteric transitions, but the pathways leading from one end state to the other are unknown. Our prime objective is to understand how protein architectures accommodate bistable structures, and what molecular motions constitute the allosteric reaction coordinates.

Hemoglobin (Hb) offers the best prospect for providing insight into the allosteric transition because new techniques and hypotheses can be tested against an extensive knowledge base. The tertiary and quaternary structure differences between the low- and high-affinity states, R and T (*2*), have been analyzed extensively (*3*). Moreover, intermediate structures can be produced with crosslinking agents (*4*), and with hybrid Hb's that mimic partially ligated forms. Thermodynamic measurements on these hybrid Hb's have uncovered intermediate states that are energetically important in the ligand binding sequence (*5*).

The allosteric transition can be studied directly by kinetic methods with the use of photodissociation of the CO adduct, HbCO, to generate unligated Hb, which then evolves from the R structure toward the equilibrium T structure before it fully recombines with the CO. Transient absorption spectroscopy has provided rate constants for several kinetic steps (*6*, *7*) subsequent to HbCO photolysis. The allosteric pathway can in principle be elucidated by determining the structures of the intermediates defined by these rate constants.

Structural information on the requisite time scales can be provided by resonance Raman (RR) spectroscopy, which can probe the protein environment of chromophoric groups through their vibrational frequencies and intensities. The technique can be applied in a time-resolved mode by means of pulsed laser excitation, and different chromophores can be selected by tuning the laser wavelength. In the case of Hb, visible excitation enhances vibrational modes of the heme group (*8*), where the primary ligation events occur, while ultraviolet excitation enhances vibrational modes of aromatic side chains, which can probe tertiary and quaternary interactions in the protein (*9*). Extensive structure-spectra correlations have been established for these chromophores, and several time-resolved resonance Raman (TR^3) studies have been performed (*9–14*). However, a full kinetic analysis has not yet been reported, either for the heme signals or for the aromatic residue signals. Using both visible and ultraviolet (UV) excitation, we have now obtained TR^3 spectra from 10 to 10^5 nanoseconds (ns) after HbCO photolysis, and have extracted the spectra of the kinetic intermediates. These spectra permit construction of a working model of the allosteric transition that involves interleaved tertiary and quaternary motions.

TR^3 spectra and kinetic analysis. The kinetic analysis relied on a set of UVRR spectra obtained with 230-nm probe pulses at a series of time delays after a 419-nm photolysis pulse. Difference spectra were generated (Fig. 1) by subtracting the spectrum of HbCO from those of the photoproduct; these transient difference spectra evolve toward the static deoxyHb minus HbCO difference spectrum. The bands are labeled according to the contributing residue type (tryptophan, W, or tyrosine, Y)

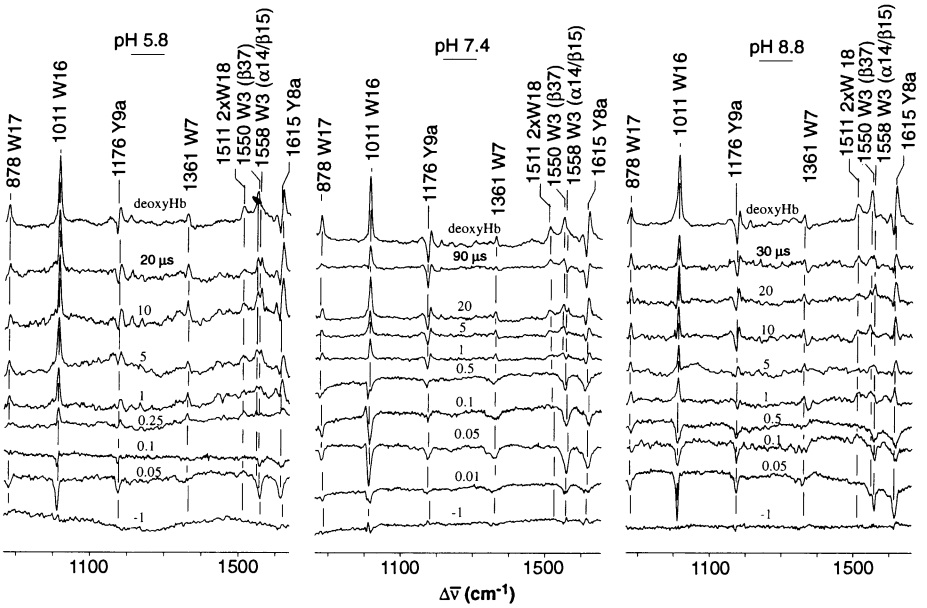

Fig. 1. The 230-nm excited (8 μJ/pulse, 300 Hz) UVRR difference spectra between the HbCO photoproduct and HbCO, at pH 5.8, pH 7.4, and pH 8.8. The delay times (μs) following photolysis of HbCO with a 419-nm (70-μJ) pump pulse are indicated. Complete photolysis was checked by monitoring the 436 nm–excited heme RR spectrum. The top spectrum is the static difference spectrum between deoxyHb and HbCO. The apparatus and techniques are described (*9*).

V. Jayaraman and T. G. Spiro are in the Department of Chemistry, Princeton University, Princeton, NJ 08544. K. R. Rodgers is in the Department of Chemistry, North Dakota State University, Fargo, ND 58105. I. Mukerji is in the Department of Biochemistry and Molecular Biology, Wesleyan University, Middletown, CT 06457.

*To whom correspondence should be addressed.

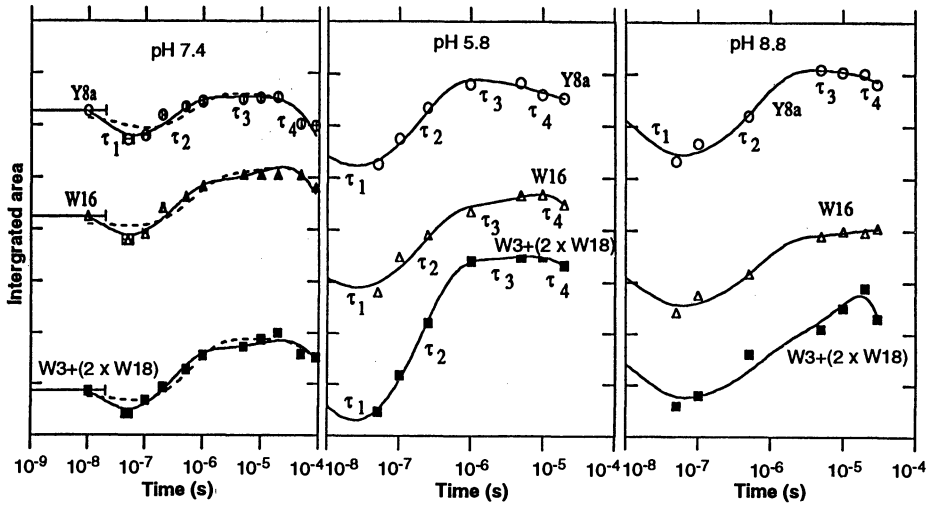

Fig. 2. Integrated peak intensities for the UVRR bands in the photoproduct spectra, at pH 5.8, pH 7.4 and pH 8.8, are plotted as a function of time. (○) Y8a band. (△) W16 band. (■) Sum of the W3 and 2×W18 bands. The data were fit (solid line) to a sum of four exponential decays (τ_1 - τ_4) with the same time constants (Table 1) for each curve. Also shown at pH 7.4 (dotted line) is the time course calculated with the time constants determined by Hofrichter *et al.* (*7*) from optical absorption transients.

Table 1. Relaxation time constants, (τ, in μs) in the HbCO photocycle, from UVRR intensity variations.

pH	τ_1	τ_2	τ_3	τ_4
5.8	0.01 ± 0.02*	0.25 ± 0.05	10 ± 1	125 ± 100†
7.4	0.02 ± 0.02	0.50 ± 0.10	17 ± 2	500 ± 500
7.4‡	0.05 ± 0.02	0.71 ± 0.14	19 ± 3	1500 ± 300
8.8	0.03 ± 0.02	0.66 ± 0.12	50 ± 5	1500 ± 500

*The uncertainties in τ_1 are due to the ~ 20-ns timing jitter between the 10-ns photolysis and probe pulses. †The uncertainties in τ_4 reflect the low amplitude of this phase because of the limited time delays (<100 μs). ‡Determined from optical absorption transient spectra by Hofrichter *et al.* (*7*).

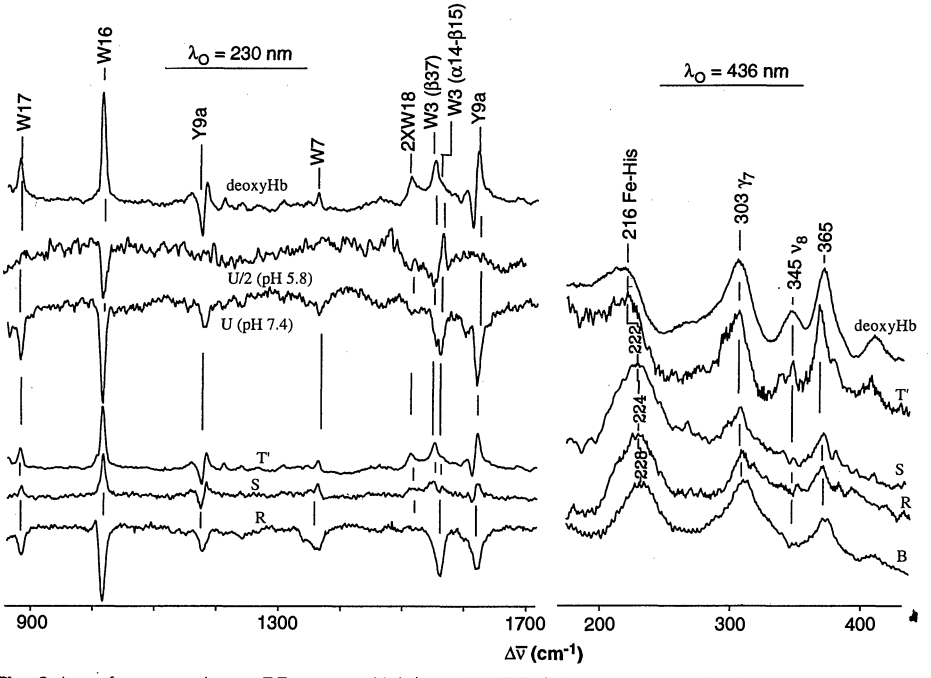

Fig. 3. Low-frequency heme RR spectra (right), and UVRR difference spectra (left) of the intermediates R-U extracted from the transient spectra; species populations were calculated with the experimental time constants. Because the time constants are well separated (by about two decades each), their uncertainties have little effect on the extracted spectra. The static spectrum (right) and difference spectrum (left) of deoxyHb are shown at the top for comparison.

and vibrational mode number, as established previously (*9*, *10*).

The time course of the spectral evolution was obtained by fitting the integrated intensities of the most prominent bands in the parent spectra, Y8, W16, and W3, to a set of four successive exponential processes (Fig. 2). The same four time constants (Table 1) accounted for all three sets of intensities, which arise from tyrosine as well as tryptophan residues. Moreover, there is satisfactory agreement with the time constants determined by Hofrichter *et al.* (*7*) from the heme optical absorption transients at pH 7.4. It is apparent that these different probes are monitoring the same set of protein intermediates.

The difference spectra of these intermediates (Fig. 3) were extracted from the transient data, with the use of the kinetic constants to calculate the population distribution at each time delay. A scheme for these intermediates, labeled R, S, T′, and U, is given in Fig. 4; we followed the convention of Frauenfelder *et al.* (*15*) so that HbCO is labeled A and the immediate photoproduct (*16*, *17*) is labeled B. No difference spectrum is shown for B because its UVRR spectrum is the same as that of HbCO; there is a definite rise time (τ_1) for the first UVRR-detectable intermediate.

Although the kinetic constants vary with pH (Table 1), the spectra of the R, S, and T′ intermediates are pH-independent. Only the spectrum of U changes between pH 5.8 and 7.4 (Fig. 3). (It could not be obtained at pH 8.8 because of low population.) The rate for the T′-U transition is known to depend on the CO concentration (*6*, *7*). Therefore, U is an intermediate in the second-order recombination of the photoproduct with CO (Fig. 4).

The 436-nm excited RR spectra of the HbCO photoproduct obtained with a 532 nm photolysis pulse (Fig. 5) revealed vibrational modes of the porphyrin ring and of the Fe-ligand bonds (*8*). Photolysis produced a deoxyheme spectrum in place of the HbCO spectrum (the 507 cm^{-1} Fe-CO stretching mode (*18*) disappeared, and the porphyrin ring stretching modes ν_2, ν_3, and ν_4 (*19*), shifted to lower frequencies), but the HbCO spectrum quickly recovered about half its amplitude, as a result of geminate recombination (from within the protein) of the photodissociated CO. The recombination yield was quantitated by deconvoluting the prominent ν_4 band into its HbCO (1372 cm^{-1}) and deoxyheme (1356 cm^{-1}) components, and normalizing their intensities with respect to HbCO and deoxyHb, measured in a separate experiment. The time course (Fig. 6) revealed a rapid geminate phase, with a yield of 55 percent, consistent with other reports (*13*, *20*). The time constant is 20 ns (solid curve), the

same as τ_1 obtained from the UVRR data (Table 1). Hofrichter *et al.* (*7*) also found that the time constant for geminate recombination and for the initial deoxyheme absorption transient are the same. We conclude that geminate recombination is coincident with the first protein conformational change.

In order to examine the evolution of the deoxyheme bands subsequent to photolysis, we subtracted the HbCO spectrum from the transient spectra with a scale factor just sufficient to eliminate the 1372 cm^{-1} ν_4 shoulder. The resulting difference bands for ν_2, ν_3, and ν_4 revealed 2 cm^{-1} downshifts in the immediate photoproduct, relative to equilibrium deoxyHb, as was reported (*14*). These shifts also relaxed in the 20-ns phase (Fig. 6). The vinyl stretching band at 1620 cm^{-1}, which was unshifted in the photoproduct and showed no evolution in time (Fig. 5), served as a control for the heme skeletal mode relaxations.

The 220 cm^{-1} band, which arose from the stretch of the Fe-histidine bonds in the deoxyheme groups, continued to change over the full time scale of the experiment (*13*) (Fig. 5). Its time course (Fig. 6) is satisfactorily described by the same four time constants as were obtained from the UVRR data. These time constants were used to extract the low-frequency deoxyheme RR spectra of the intermediates R-T′ from the transient spectra (Fig. 3); in this case the spectrum of B is also reported, since the deoxyheme spectrum was detected in the immediate photoproduct. The Fe-His stretching frequency shifted from 228 to 224 to 222 to 216 cm^{-1} in B through T′, ending up at the same frequency as in deoxyHb. The 345 cm^{-1} porphyrin substituent bending mode ν_8, which was missing in the immediate photoproduct (*13*), reappeared only on formation of T′.

Nature of the intermediates. In deoxyHb, the heme is five-coordinate and high-spin, with the Fe lying above a domed porphyrin, and connected to the proximal histidine by a bond that is tilted relative to the heme normal (Fig. 7) (*3*). Ligation produces a six-coordinate low-spin heme, with short perpendicular bonds to Fe, which becomes centered in a flattened porphyrin. This stereochemical change is accompanied by tertiary structure alterations, the most prominent of which is a shift of the proximal F helix across the face of the heme (*3*). This shift is believed to induce dimer rotation (*21*), which is the most striking change between the T and R structures (*3*), because the altered interdimer contacts mostly involve the FG corners and C helices on opposite chains (Fig. 7). As a result of this rotation, a number of H bonds and salt bridges, which stabilize the T structure, are broken. These structural considerations provide the context for interpreting the RR spectra of the intermediates. The 55 percent geminate recombination yield means that half the chains, on average, are ligated in the intermediates R, S, and T′ (Fig. 4) although it is not known whether the ligands are distributed randomly or in a chain-selective fashion (see discussion of T′ below.)

In B, the immediate photoproduct, the Fe-CO bond is broken (*16*, *17*). By analogy with the B state of MbCO (Mb, myoglobin), the CO is expected to take up a well-defined position in the heme pocket, in which its orientation is perpendicular to the bound CO in A (*22*). In recent x-ray structures of MbCO crystals that were photolyzed at 4 K, the CO is seen lying over

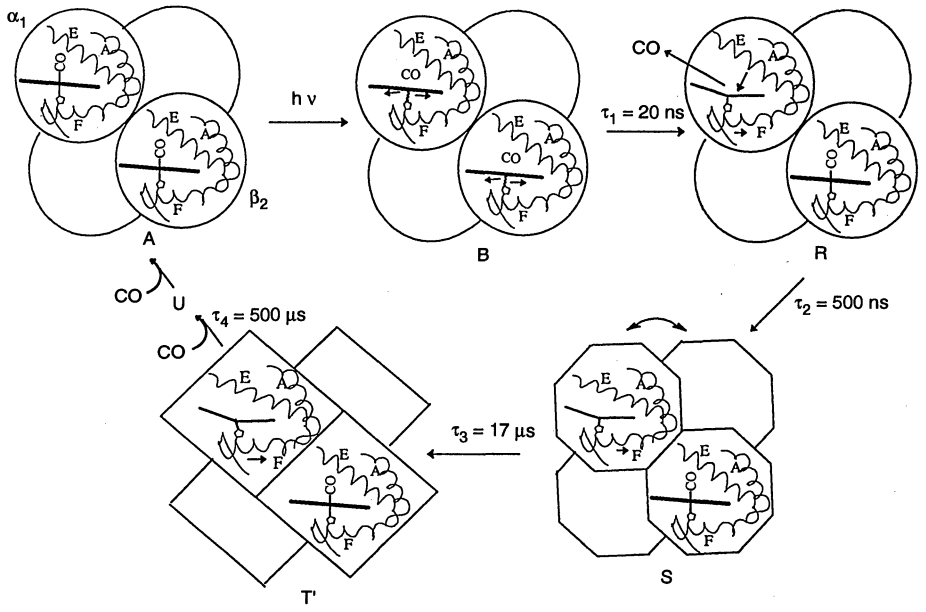

Fig. 4. Model of the Hb reaction coordinate. Photolysis of HbCO (A) produces the geminate state (B), and then intermediates S-U, with the indicated time constants (pH 7.4). Arrows in the tetramer indicate motions proposed on the basis of the TR^3 spectra. Religation is indicated for half the subunits in R, S, and T′.

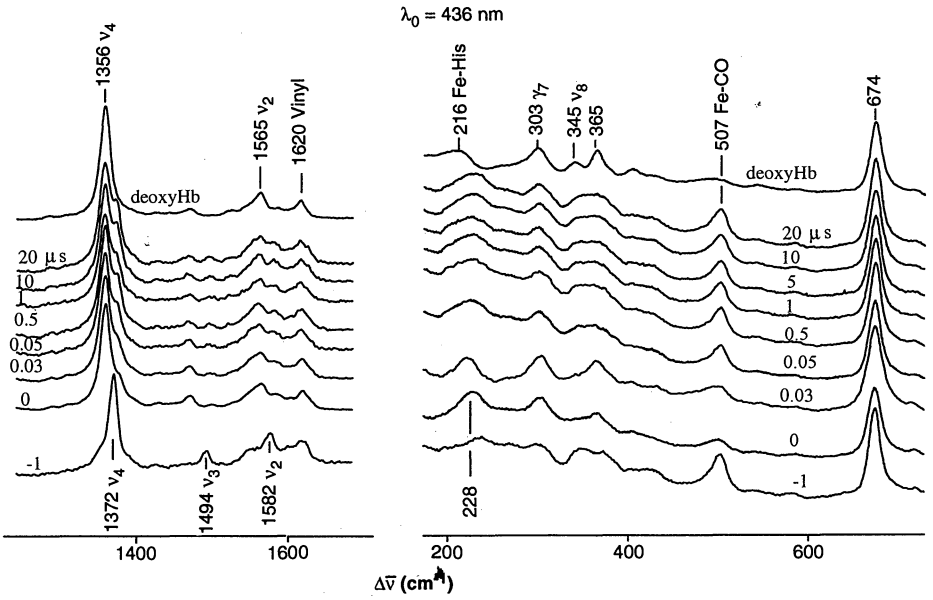

Fig. 5. The 436-nm (10 μJ per pulse, 300 Hz) excited resonance Raman spectra of the photoproducts of HbCO, generated at the indicated times after a 532-nm (150-μJ) photolysis pulse and of deoxyHb (top). Photodissociation and geminate recombination of the CO are seen in the loss and recovery of the 1375 cm^{-1} ν_4 ring-stretching band of HbCO, and of the 507 cm^{-1} Fe-CO stretching band. The pulse-probe apparatus was similar to that used for the UVRR experiments, except that a triple spectrograph with a diode array detector was used to collect the spectra.

one of the pyrrole rings of the heme (*23*, *24*). The Fe atom is displaced from the heme plane, in this structure, but only by about 80 percent of the displacement seen in deoxyMb (*23*), a value in excellent agreement with the 75 percent estimate derived from the core-size marker band (ν_2, ν_3) RR shifts in the immediate photoproduct of HbCO (*14*). The retardation of this displacement is attributed to constraint by the proximal histidine, which is attached to the F helix. The nonbonded forces impelling the high-spin Fe out of the heme plane (*25*), together with the restraint provided by the F helix, produce a compression of the Fe-His bond, as seen in its elevated frequency (228 cm^{-1}) relative to the value expected in a relaxed deoxy structure (220 to 222 cm^{-1} for deoxyMb or modified deoxyHb's in the R state) (*26*).

The absence of changes in the UVRR spectra between A and B suggests that there are no large-scale protein motions at this early stage of the reaction coordinate. This would be consistent with the photoproduct energy being stored in the heme pocket, ready to propagate further in the next intermediate.

The first indication of protein structure change occurred in the 20-ns transition from B to R. The UVRR difference spectrum of R is characteristic of Hb tetramers which are in the R quaternary state but which have one or more deoxyhemes [for example, tetramers having one deoxyheme and three cyanomethemes (*27*), or tetramers having two FeCO-hemes and two unligated cobalt-containing hemes (*10*)]. The spectrum contains strongly negative tryptophan bands, and the position of W3 identifies the contributing residues as the interior tryptophans, α14 and β15 (*9*). These residues are on the A helices but bridge to the E helices via H bonds to the OH groups of the E helix residues $Thr^{\alpha 67}$ and $Ser^{\beta 72}$ (Fig. 7). The intensity loss in all the Trp bands indicates a weakening of these H bonds via increased separation of the A and E helices (*10*). This increased separation is suggested to be a natural consequence of E helix displacement toward the heme when there is no ligand in the heme pocket, but the tetramer remains in the R state (Fig. 4).

The visible RR spectra showed the heme structure to be relaxed in the R intermediate; the porphyrin core size marker frequencies have attained their deoxyHb values, signaling full out-of-plane displacement of the Fe atom, while the Fe-His frequency has decreased from 228 to 224 cm^{-1}, only slightly higher than the value expected for a relaxed deoxyheme structure (*26*). We infer that the energy stored in B, at the Fe-His bond and its connection to the F helix, is transmitted via the EF corner to the E helix during the B→R transition. The resulting displacement of the E helix pushes the CO out of the heme pocket in half the chains but induces rebinding of the CO in the other half. This mechanism accounts for the coincidence of the time constants for the first UVRR transient and for geminate rebinding. The spectroscopic indications are that the intermediate R is genuinely an R state tetramer, in which CO is bound to the heme in half the chains on average and is absent from the heme pocket in the other half.

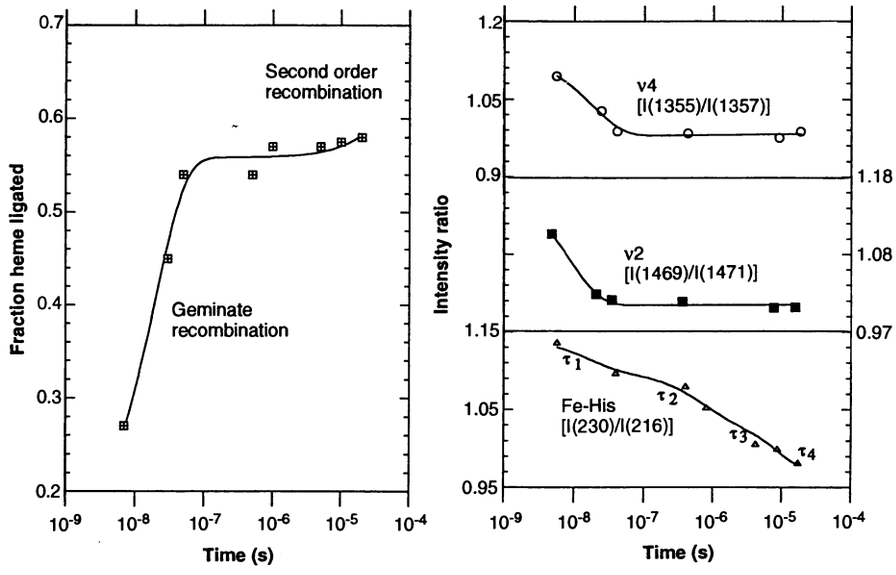

Fig. 6. (Left) Time course of the fraction of hemoglobin molecules that have recombined after photolysis. The solid curve is drawn with the time constants τ_1 (20 ns) for the geminate phase, and τ_4 (500 μs) for the second order phase. (Right) Intensity ratios for the prompt and late positions of the deoxyheme ν_2 (■) and ν_4 bands (○), and the Fe-His (△) band. The solid curves were drawn with the time constant τ_1 (20 ns) for ν_2 and ν_4, and with the τ_1- τ_4 time constants (Table 1) for the Fe-His band.

The E helix displacement is a transient phenomenon. By the time R evolves to S, with a 0.5-μs time constant, the negative UVRR difference bands of $Trp^{\alpha 14}$ and $Trp^{\beta 15}$ have disappeared (Fig. 3). They are replaced by the same bands that are seen in the static deoxyHb difference spectrum, but with much lower amplitude. The static difference spectrum results mainly from altered contacts at the $\alpha_1\beta_2$ interface, especially the strong T state H bonds of $Tyr^{\alpha 42}$ and $Trp^{\beta 37}$ (*9*) (Fig. 7), which are broken in the R state because of the rotation between dimers (*3*). It has been assumed (*6*, *7*) that the quaternary rearrangement of the subunits takes place in the final kinetic phase of the protein, the ~ 20-μs phase leading to the species we have labeled T′. Our evidence, however, implicates R→S as the quaternary transition because the difference

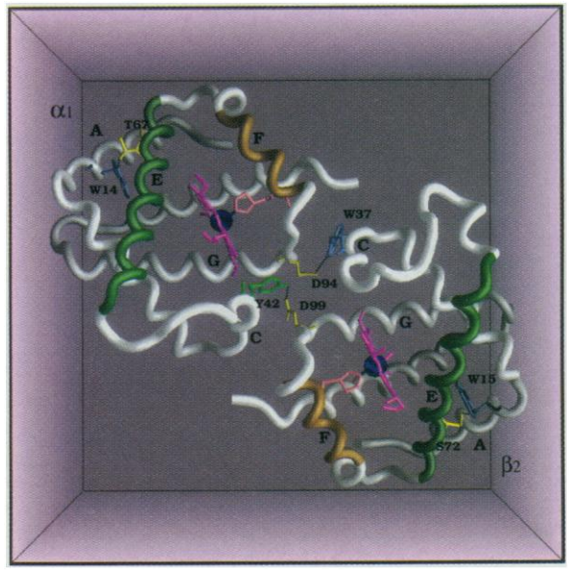

Fig. 7. Helix diagram (from Brookhaven data bank coordinates) of the α_1 and β_2 subunits of deoxyHb, showing the interface contacts involving $Tyr^{\alpha 42}$ (green) and $Trp^{\beta 37}$ (blue), and the H-bonding interactions of the interior Trp residues α14 and β15 (blue). The E (green) and F (brown) helices are highlighted as are the heme groups and proximal histidine side chains (pink), bound to the Fe atoms (purple). The $\alpha_1\beta_2$ contacts are altered in the T-R transition via interdimer rotation.

UVRR spectrum of S shows that the $Tyr^{\alpha 42}$ and $Trp^{\beta 37}$ H bonds have begun to form, albeit weakly. Since these contacts are in two distinct regions of the $\alpha_1\beta_2$ interface (Fig. 7), the S intermediate must have a quaternary structure with a T-like orientation of the dimers.

The $\alpha_1\beta_2$ contacts involve residues on the C helix of one chain and on the FG corner of the other. It therefore seems likely that the dimer rotation and the E helix restoration are both driven by displacement of the F helix toward the EF corner, the direction seen in deoxyHb, relative to ligated structures (*3*). However, this displacement can only be partial in the S intermediate because the Fe-His stretching frequency is 222 cm^{-1}, a typical value for a relaxed deoxyheme, and significantly higher than the 216 cm^{-1} value of deoxyHb. We infer that S retains an R-like tertiary structure even after having undergone the subunit rearrangement that leads to the T state.

T-like properties are finally produced in the S→T′ transition. The low-frequency heme RR spectrum of T′ (Fig. 3) is the same as that of deoxyHb, including the appearance of the 345 cm^{-1} ν_8 band and broadening and lowering of the Fe-His band to 216 cm^{-1}. The difference UVRR spectrum has all the features of the deoxyHb spectrum and is substantially stronger than the spectrum of S. We conclude that the $\alpha_1\beta_2$ contacts are strengthened in T′ as a result of further tertiary changes that weaken the Fe-His bond. These further changes no doubt involve a final shift of the F helix, in view of the tilting and reorientation of the proximal imidazole ligand seen in the deoxyHb structure (*3*). The likely role of these structural features in producing the depressed Fe-His frequency of deoxyHb has been discussed extensively (*25, 26, 28*).

Despite these T-like properties, T′ is not fully in the T state. The amplitude of the difference UVRR spectrum, although stronger than that of S, is weaker (60 percent) than that of deoxyHb (Fig. 3). This lower amplitude implies a weakening of the $\alpha_1\beta_2$ H bonds, relative to deoxyHb, an effect attributable to the two bound CO ligands per tetramer. The amplitude is the same as has been found for asymmetrically diligated cyanometHb hybrid, in which the cyanomethemes are in the $\alpha_1\beta_1$ (or equivalently $\alpha_2\beta_2$) dimer (*27*). In contrast, the symmetrically di-ligated hybrids (cyanomethemes in the two α or in the two β chains), give different spectra; they are superpositions of T minus R contributions and R_{deoxy} contributions, reflecting a mixture of T and R tetramers (*29*). Neither the symmetrically di-ligated hybrids nor the T′ intermediate have R_{deoxy} contributions.

The asymmetrically di-ligated cyanometHb hybrid species represents a third cooperativity state (*5*). Its free energy of dimer-to-tetramer assembly is 3 kcal/mol less than that of deoxyHb, but also 3 kcal/mol greater than the symmetrically di-ligated hybrids, and is in gross violation of the two-state model (*30*). Similar free energy differences have been obtained for other hybrid systems, all of which implicate at least one cooperativity state in addition to the classical T and R states (*5*). The T′ state is inferred to have a deformed $\alpha_1\beta_2$ interface, with weakened $Trp^{\beta 37}$ and $Tyr^{\alpha 42}$ H bonds (*27*), as a result of the forces generated by the binding of two ligands to the same dimer. This is the dominant species present after the final protein relaxation because tetramers with two ligands on the same dimer are more stable than those with the two ligands on opposite dimers (*5*). Whether the CO's are on the same or different dimers in the earlier intermediates, R and S, is uncertain; the 17-μs rise time of T′ is probably long enough for ligand interchange among the chains within a tetramer.

The $\alpha_1\beta_2$ interface deformation in T′ is without effect on the Fe-His bond strength, which is the same as in deoxyHb, as judged by the RR frequency. Thus, Hb retains a T-like tertiary structure for the unligated chains even when two ligands are bound to the tetramer; evidently the $\alpha_1\beta_2$ interface is able to accommodate the entire binding-induced strain.

Second-order recombination with CO returns the Hb photoproduct to HbCO, but an additional intermediate, U, is formed en route, as revealed by changes in the UVRR spectra. Since the T′ precursor has two bound CO's on average, U must consist predominantly of tri-ligated tetramers. At pH 7.4, the spectrum is the same as that observed for the R intermediate; it is an R_{deoxy} spectrum, with negative peaks (Fig. 3). This spectrum is consistent with the expected switch from the T to the R quaternary structure on binding a third ligand; the negative peaks arise from the E helix displacement in the one remaining unligated subunit. At pH 5.8, the spectrum of U still contains a negative difference band for W16, but the W3 signal, which is at the $Trp^{\alpha 14}$ and $Trp^{\beta 15}$ position, is now positive. This positive peak may result from stabilization of the T quaternary structure at low pH, even when three ligands are bound on average. A similar feature was seen in the difference spectrum of fluorometHb with and without the allosteric effector molecule IHP (*31*), and was suggested to result from a strengthening of the $Trp^{\alpha 14}$ and $Trp^{\beta 15}$ H bonds in ligated chains within the T state.

With the exception of U, the UVRR difference spectra of all the intermediates are independent of pH, despite the altered time constants. Thus, the mechanism of the allosteric transition does not change with pH. In particular, the amplitudes of the signals for T′ are unchanged when the pH is raised or lowered from 7.4, implying the presence of asymmetrically di-ligated species at all pH values. The retention of two ligands, on average, is consistent with the finding (*20*) that the geminate recombination yield is the same at pH 9 as at pH 7.

The time constants for the steps in the pathway increase with increasing pH (Table 1). This trend is consonant with the finding (*13*) that the Fe-His frequency evolves faster at low pH, and with the observation (*32*) of faster UVRR changes at low pH. For τ_1 and τ_4, the changes are within the experimental uncertainties, but for τ_2 and τ_3 the effect is real. Both of them double between pH 5.8 and 7.4; between pH 7.4 and 8.8, τ_3 triples, while τ_2 increases modestly. The speeding up of the protein rearrangement as the pH is lowered implicates the same interactions for the intermediates as are responsible for the well-known stabilization of the T state at low pH (*1*). These interactions are important for τ_2, which we interpret as the subunit rearrangement phase, as well as τ_3, during which the T′ state is locked in.

The allosteric reaction coordinate. On the basis of the structural information provided by the TR^3 spectra we propose a model for the HbCO photocycle (Fig. 4), which contains the following features:

1) Photolysis produces the geminate state, B, in which the dissociated CO is trapped in the heme pocket. The F helix restrains the Fe out-of-plane displacement, compressing the Fe-His bond and expanding the porphyrin core.

2) Some 20 ns later, the strain at the F helix-heme connection relaxes and is transmitted to the E helix. The result is CO recombination for half the chains and CO expulsion from the other half, as the E helix is displaced toward the heme. At this stage, the protein is in the R state.

3) In the next step, which occurs with a 0.5-μs time constant, the E helix is repositioned, probably via a shift in the F helix, and the dimers rotate into position to begin forming the $\alpha_1\beta_2$ contacts. The Fe-His bond remains relaxed (intermediate S).

4) In the 17-μs phase, the Fe-His bond becomes strained, as in deoxyHb, when the $\alpha_1\beta_2$ contacts lock into place. However, the resulting molecule is in the T′ state, in which the interface contacts are weakened relative to the T state, because two ligands, on average, remain bound in the tetramer; these ligands occupy the α and β chains in a single dimer. The rate of formation for both S and T′ increases with decreasing pH, as a result of the proton-linked interactions which are known to stabilize the T state at low pH.

5) The binding of a third ligand via

second-order recombination (intermediate U) converts the molecules to the R state at pH 7.4; the remaining deoxy chain produces a R_{deoxy} UVRR difference spectrum. At pH 5.8, however, the tri-ligated molecules probably remain in the T quaternary structure and produce a positive W3 UVRR difference band for the interior tryptophan residues.

The most interesting conclusion to emerge from this study is that the allosteric reaction coordinate is not unidirectional, but instead proceeds by reciprocating tertiary and quaternary motions. Although the force generated by ligand dissociation is initially felt at the proximal His residue, the first large-scale protein motion (20 ns) involves the E helix, on the distal side of the heme. The next step (0.5 μs) is dimer rotation and the initial formation of the quaternary H bonds. The last step (17 μs) completes the circuit, locking the quaternary contacts into place and shifting the proximal F helix to its deoxyHb position, thereby straining the Fe-His bond.

This strain is critical to cooperative ligand binding because it is responsible for lowering the affinity in the T state. The oxygen affinity has been directly linked to the Fe-His stretching frequency in various Hb's (*32*) as has the activation energy for CO rebinding (*13*, *26*). Likewise, Gibson's transition from fast to slow recombining Hb (*5*) is shown by the present work to be a transition (S→T′) from a relaxed to a strained Fe-His bond. This transition establishes the coupling of the ligation free energy to protein structure change, but it is mainly a tertiary, not a quaternary motion, in that the interdimer rotation has already occurred in S.

REFERENCES AND NOTES

1. M. F. Perutz, *Mechanisms of Cooperativity and Allosteric Regulation in Proteins* (Cambridge Univ. Press, Cambridge, 1990).
2. J. L. Monod, J. Wyman, J. P. Changeux, *J. Mol. Biol.* **12**, 88 (1965).
3. J. Baldwin and C. J. M. Chothia, *ibid.* **129**, 175 (1979).
4. S. Miura and C. Ho, *Biochemistry* **21**, 6280 (1982); M. A. Schumacher *et al.*, *Nature* **375**, 84 (1995).
5. G. K. Ackers, M. L. Doyle, D. Myers, M. A. Daugherty, *Science* **255**, 54 (1992).
6. C. Sawicki and Q. H. Gibson, *J. Biol. Chem.* **251**, 1533 (1976).
7. J. Hofrichter, J. H. Sommer, E. R. Henry, W. A. Eaton, *Proc. Natl. Acad. Sci. U.S.A.* **80**, 2235 (1983).
8. D. L. Rousseau and J. M. Friedman, *Biological Applications of Raman Spectroscopy*, T. G. Spiro, Ed. (Wiley, New York, 1987), vol. 3, p. 133.
9. K. R. Rodgers, C. Su, S. Subramaniam, T. G. Spiro, *J. Am. Chem. Soc.* **114**, 3697 (1992).
10. K. R. Rodgers and T. G. Spiro, *Science* **265**, 1697 (1994).
11. S. Kaminaka, T. Ogura, T. Kitagawa, *J. Am. Chem. Soc.* **112**, 23 (1990).
12. J. M. Friedman and K. B. Lyons, *Nature* **284**, 570 (1980).
13. T. W. Scott and J. M. Friedman, *J. Am. Chem. Soc.* **106**, 5677 (1984).
14. S. Dasgupta and T. G. Spiro, *Biochemistry* **25**, 5941 (1986).
15. P. Ormos *et al.*, *Proc. Natl. Acad. Sci. U.S.A.* **85**, 8492 (1988).
16. B. Locke, I. Lian, R. M. Hochstrasser, *Chem. Phys.* **158**, 409 (1991).
17. P. A. Anfinrud, C. Han, R. M. Hochstrasser, *Proc. Natl. Acad. Sci. U.S.A.* **86**, 8387 (1989).
18. E. A. Kerr and N. T. Yu, in *Biological Applications of Raman Spectroscopy*, T. G. Spiro, Ed. (Wiley, New York, 1987), vol. 3, p. 39.
19. T. G. Spiro, in *Iron Porphyrins*, part 2, A. B. P. Lever and H. B. Gray, Eds. (Addison-Wesley, Redding, MA, 1983), pp. 89–160.
20. S. Pin, P. Valat, H. Tourbez, B. Alpert, *Chem. Phys. Lett.* **128**, 79 (1986).
21. B. R. Gellin and M. Karplus, *J. Mol. Biol.* **171**, 489 (1983).
22. M. Lim, T. A. Jackson, P. A. Anfinrud, *Science* **269**, 962 (1995).
23. I. Schlichting, J. Berendzen, G. N. Phillips, R. M. Sweet, *Nature* **371**, 808 (1994).
24. T. Y. Teng, V. Srajer, K. Moffat, *Nature Struct. Biol.* **1**, 701 (1994).
25. J. M. Friedman, D. L. Rousseau, M. R. Ondrias, R. A. Stepnoski, *Science* **218**, 1244 (1982).
26. J. M. Friedman, T. W. Scott, R. A. Stepnoski, M. Ikeda-Saito, T. Yonetani, *J. Biol. Chem.* **258**, 10564 (1983).
27. V. Jayaraman and T. G. Spiro, *Biochemistry* **34**, 4511 (1995).
28. O. Bangcharoenpaurpong, K. T. Schomacker, P. M. Champion, *J. Am. Chem. Soc.* **106**, 5688 (1984).
29. I. Mukerji and T. G. Spiro, *Biochemistry* **33**, 13132 (1994).
30. G. K. Ackers, *Biophys. Chem.* **37**, 371 (1990).
31. V. Jayaraman, K. R. Rodgers, I. Mukerji, T. G. Spiro, *Biochemistry* **32**, 4547 (1993).
32. S. Kaminaka and T. Kitagawa, *J. Am. Chem. Soc.* **114**, 3256 (1992).

33. We thank Professors Gary Ackers and Philip Anfinrud for helpful discussions and Beth Villafennea for creating Fig. 7. Supported by NIH grant GM 25158.

20 December 1994; accepted 21 August 1995